IEEE Access
Multidisciplinary | Rapid Review | Open Access Journal

Received December 10, 2020, accepted December 23, 2020, date of publication December 29, 2020, date of current version January 13, 2021.

Digital Object Identifier 10.1109/ACCESS.2020.3047732

Batteries State of Health Estimation via Efficient Neural Networks With Multiple Channel Charging Profiles

NOMAN KHAN[1], (Student Member, IEEE), FATH U MIN ULLAH[1], (Student Member, IEEE), AFNAN[2], AMIN ULLAH[1], (Member, IEEE), MI YOUNG LEE[1], (Member, IEEE), AND SUNG WOOK BAIK[1], (Senior Member, IEEE)

[1]Sejong University, Seoul 143-747, Republic of Korea
[2]Digital Image Processing Laboratory, Islamia College Peshawar, Peshawar 25120, Pakistan

Corresponding author: Sung Wook Baik (sbaik@sejong.ac.kr)

This work was supported in part by the Korea Institute of Energy Technology Evaluation and Planning and the Ministry of Trade, Industry Energy, Republic of Korea (Development and Demonstration of Real-time Monitoring Platform regarding EES Operation Status for Safety Enhancement), under Grant 20209810300090, and in part by the National Research Foundation of Korea Grant funded by the Korea government (MSIT) under Grant 2019M3F2A1073179.

ABSTRACT The prognostics and health management (PHM) plays the main role to handle the risk of failure before its occurrence. Next, it has a broad spectrum of applications including utility networks, energy storage systems (ESS), etc. However, an accurate capacity estimation of batteries in ESS is mandatory for their safe operations and decision making policy. ESS comprises of different storage mechanisms such as batteries, capacitors, etc. Consequently, the measurement of different charging profiles (CPs) has a strong relation to battery capacity. These profiles include temperature (T), voltage (V), and current (I) where the CPs patterns vary as the battery ages with cycles. Consequently, estimating a battery capacity, the conventional methods practice single channel charging profile (SCCP) and hop multiple channel CPs (MCCPs) that cause incorrect battery health estimation. To tackle these issues, this article proposes MCCPs based battery management system (BMS) to estimate batteries health/capacity through the deep learning (DL) concept where the patterns in these CPs are changed as the battery ages with time and cycles. Thus, we deeply investigate both machine learning (ML) and DL based methods to provide a concrete comparative analysis of our method. The adaptive boosting (AB) and support vector regression (SVR) are widely compared with long short-term memory (LSTM), multi-layer perceptron (MLP), bi-directional LSTM (BiLSTM), and convolutional neural network (CNN) to attain the appropriate approach for battery capacity and state of health (SOH) estimation. These approaches have a high learning capability of inter-relation between the battery capacity and variation in CPs patterns. To validate and verify the proposed technique, we use NASA battery dataset and experimentally prove that BiLSTM outperforms all the approaches and obtains the smallest error values for MAE, MSE, RMSE, and MAPE using MCCPs compared to SCCP.

INDEX TERMS Battery management system, bi-directional LSTM, capacity, deep learning, energy storage systems, ensemble learning, lithium-ion battery, machine learning, renewable energy sources, smart grid, state of health, transfer learning.

NOMENCLATURE

ACRONYMS

ANN	Artificial neural network
AN	Artificial neuron
AB	Adaptive boosting
BMS	Battery management system
BiLSTM	Bi-directional LSTM
BESS	Battery energy storage system
CPs	Charging profiles
CNN	Convolutional neural network
DL	Deep learning
ESS	Energy storage systems

The associate editor coordinating the review of this manuscript and approving it for publication was Sanjeevikumar Padmanaban.

ECM	Equivalent circuit model
EM	Electrochemical model
MLP	Multi-layer perceptron
MSE	Mean square error
ML	Machine learning
MAE	Mean absolute error
PHM	Prognostics and health management
PFM	Particle filtering model
POS	Performance of stumps
RMSE	Root mean square error
RES	Renewable energy sources
RNN	Recurrent neural network
RUL	Remaining useful life
SVR	Support vector regression
FFNN	Feedforward neural network
LSTM	Long short-term memory
Li-ion	Lithium-ion
MCCPs	Multiple channel charging profiles
MAPE	Mean absolute percentage error
SOH	State of health
SCCP	Single channel charging profile
SVM	Support vector machine
UKF	Unscented kalman filter

I. INTRODUCTION

Renewable energy sources (RES) are important for continuous energy supply through modern smart grids. Due to the large population, fast economic growth, and development in market economies, the global energy demand is growing rapidly. However, the required energy for industries and households in these days greatly depends on fossil fuels. Many problems and challenges are arisen for the operators in the smart grids such as increase in the frequency variation, reduction in the transient voltage (V) and reliability, and decrease in power quality due the enlarged penetration of unreliable and unbalanced RES [1]. These issues can be handled through separating energy demands from energy generation with the help of efficient energy storage systems (ESS) approach. Additionally, the issues in quality of power system can be solved with the help of ESS by providing auxiliary facilities. For instance, peak cutting, leveling of load, avoidance of triad, and regulation of frequency [2]. Superconducting magnetic storage, hydrogen, compressed air, pumped hydro, cryogenic, flywheel, and fuel cells are the essential forms of ESS. In ESS, the battery energy storage system (BESS) has several advantages such as small amount of conditions maintenance, quick response, storage size, rate of discharging, long-life cycle, high ability of charging and discharging rates, and effective energy. Nowadays, batteries price is declining that results in raising several opportunities for cost effective applications in large scale modern grid. In order to balance the energy demand and its supply, BESS uses frequency reaction facilities, loop of peak power, and support for voltage. Several mechanisms in batteries all over the world are settled to support the modern grid.

The prognostics and health management (PHM) plays an important role for fault prediction that has high chance of occurrence in different real-world applications such as industries, space missions, electronic appliances, and BESS [3], [4]. The prognostic analysis is the fault prediction based on future condition estimation, error indications, and the remaining useful life (RUL) [5]. Preliminary actions are taken in order to control the situation in the applications rather than just responding to the fault after its occurrence. PHM also allows a system just in time to report the performance loss from which the affected components of a system can be replaced until it affects the overall performance of the system. PHM can notify the effective period of a component that work in an application. Accurate prediction of the performance level of the components is essential for effective actions in case of fault occurrence.

Batteries such as Lithium-ion (Li-ion) are extensively utilized in movable electrical appliances such as cellular phones, smart watch, and smart tablet etc., and other systems including automobiles, aerospace systems, and BESS. Li-ion batteries are rechargeable, having high energy power, and long-term life cycle [6], [7]. The performance of these types of rechargeable batteries is degraded with the passage of time. In batteries, electric energy is produced with the help of electrochemical reactions. As a battery is repeatedly charged and discharged, the total effective battery state of health (SOH) and capacity decrease. With the passage of time, the output power of battery is affected which results in performance degradation. This is the main factor to be consider in the case of batteries to prevent system failure or explosion due to battery failure. For device operation, accurate prediction of the efficient performance and SOH of batteries is very critical. In order to prevent system failure, the batteries performance should be identified to ensure the capability of serving in any condition.

There are several examples such as the vehicles lifecycle, buildings, bridges, etc. For instance, the SOH of different parts of the vehicle engine, the car condition, and its performance can be predicted. Before any fault or accident, it can be properly maintained. Similarly, when the life time of the materials used in the construction of the buildings and bridges completed, they become dangerous for living society [8]. So, in this case the SOH estimation helps in safety measures. These ideas inspire us to focus on the efficient SOH and RUL prediction of the batteries. We use data from the battery management system (BMS) of different charging profiles (CPs) of Li-ion batteries. Several studies in the literature are discussed and implemented different techniques for the SOH estimation and level of capacity degradation. The techniques employed for the prediction are mainly based on two different approaches, including model-based and data driven-based methods. We overview the literature about these approaches in the following sections.

A. MODEL-BASED APPROACHES

The two significant mechanisms are commonly used in model-based approaches for SOH and power estimation of batteries; that are Equivalent circuit model (ECM) and electrochemical model (EM). For instance, Goebel *et al.* [9] analyzed the EM and examined the health of a battery using data from ''Gen 2'' Li-ion cells. They utilized several approaches for the problem solution and ranked particle filter based technique at the top. Similarly, Daigle and Kulkarni [10] utilized electrochemistry based models and developed a technique for accurately prediction of time for the effective charge used in batteries and the extinction time of a battery. Next, Safari and Delacourt [11] proposed a study of the capacity loss mechanism of the graphite/LiFePO4 commercial cell.

They employed the single particle model to understand the battery loss capacity during storage and consumption of the charge. Besides, Zhang *et al.* [12] focused on to improve the performance of a battery and to decrease the overall price of ESS. Similarly, Hu *et al.* [13] proposed a technique to estimate the SOH and to predict the RUL of medical instruments batteries. They exploited the approach of gauss hermite particle filter for prediction purpose. Likewise in another work of Hu *et al.* [14], a hybrid approach based on data driven model is introduced to predict the SOH and to predict the RUL of the Li-ion batteries installed in medical appliances. These techniques are quite helpful and gives a basic understanding of the electrochemical reactions took place in a battery. However, the techniques discussed above are still in use but, these approaches are high computationally expensive due to solving and using some partial differential equations. Compared to the EM, the computational complexity of the ECM is relatively low and only applied to minimal operating conditions when parameters are defined.

B. DATA DRIVEN-BASED APPROACHES

Model-based approaches have some limitations that are overcome with the help of data driven-based approaches. These approaches are based on artificial intelligence and have gained a great attention due to their effective role in the SOH estimation. In real-time battery SOH and capacity level of degradation estimation, several data driven-based approaches are applied. For effective battery life estimation, Liu *et al.* [15] utilized the unscented particle filter approach employing discharging voltage and time measurements. Similarly, for effective management of Li-ion batteries in electrical automobiles, Plett [16] utilized extended kalman filtering based approach. Next, Guha and Patra [17] used particle filtering model (PFM) to estimate the capacity of Li-ion batteries utilizing test data. Furthermore, for the SOH estimation of batteries, Walker *et al.* [18] tested two approaches of PFM including unscented kalman filter (UKF) and nonlinear least squares. Amongst these, they ranked PFM at the top due to its accurate prediction. In another study, Zheng and Fang [19] utilized UKF along with relevance vector regression and efficiently predicted life time of Li-ion batteries. Data driven-based several ML approaches such as relevance vector machine, support vector machine (SVM), ensemble learning, feed forward neural network (FFNN), etc., and DL approaches such as LSTM are also utilized [20], [21]. For instance, Liu *et al.* [22] utilized the SVM approach and predicted the remaining life time with high precision of the Li-ion battery. A research presented in [23] proposed a real-time approach for battery health prediction, that is based on FFNN by using voltage curves of the battery. Similarly, You *et al.* [24] employed recurrent neural network (RNN) for battery state estimation in electric vehicles. They used sequential data of current and voltage of batteries. Furthermore, Hu *et al.* [25] introduced an approach where sparse Bayesian predictive modelling and sample entropy of voltage were combined. They exploited the data of multiple Li-ion batteries varying temperature and experimentally showed the effectives of the proposed technique. Shen *et al.* [26] used deep CNN to estimate the capacity level of Li-ion batteries considering measurements of voltage, charge capacity, and current. Severson *et al.* [27] utilized elastic net that is based on the features of discharge voltage curves, temperature, and coefficient of internal resistance in batteries. Consequently, Richardson *et al.* [28] employed a data driven-based approach using Gaussian process regression methods to predict batteries capacity. Another method presented by Shen and Khaligh [29] proposed a dynamic programming approach for the energy management system to increase the lifetime of batteries for efficient performance. Bole *et al.* [30] employed kalman filtering algorithm and predicted the internal state of the battery. He *et al.* [31] applied artificial neural Network (ANN) along with kalman filter for the battery state of the charge estimation. Similarly, Reihani *et al.* [32] used linear regression and other optimization algorithms for efficient battery energy management systems. Lee *et al.* [33] provided a data driven-based model that takes into account battery degradation during the discharge and charge phase.

In BMS, the signals noise interaction and its expected effects on the unbiased parameters of the battery model are important to be considered and to deal the noise corruption problems. Researchers have applied several techniques to handle this problem. For instance, Wei *et al.* [34] proposed a hybrid approach of least square regression and variable projection to estimate the noise disturbance and model impartial parameters. Next, they incorporated gauss newton based numerical solver to improve the computational efficiency. Similarly, Wei *et al.* [35] estimated the battery state of charge and capacity using kalman filter and recursive least squares while Shen *et al.* [36] used a deep neural network with transfer learning approach and applied ensemble learning mechanisms to predict the capacity of batteries. Wang *et al.* [37] emphasized the role of battery modeling and state estimation in power energy storage and management by analyzing different approaches. Further, Garg *et al.* [38] proposed a genetic programming approach using the temperature and discharging rate as input parameters. However, ML techniques have successfully contributed to the battery SOH and capacity estimation using battery data [39]. For instance,

Garge *et al.* [40] presented a robust and dynamic automated ANN based approach for capacity prediction of Li-ion batteries. This capacity helped to efficiently estimate the SOH of batteries fixed in hybrid electric vehicles to predict the travel range and energy storage capability [41]. Thus, a robust and efficient battery health and level of degradation prediction systems are required to efficiently control power storage systems [42].

For effective prediction of the level of battery performance and life time estimation, data driven-based approaches are quite easy and efficient. They are very simple as compared to model-based methods, inexpensive in terms of computations and easy to implementation. Inspired by data driven-based techniques, we propose a novel comparative framework based on ML and DL approaches exploiting MCCPs of Li-ion batteries that are, voltage, current, and external temperature. The contributions of the proposed method are summarized as follows:

- The data obtained from BMS contain abnormalities such as null values, outliers, etc. To tackle these issues, we apply a preprocessing step to remove the null values and to normalize the raw data in the range of 0 and 1.
- Existing literature focuses and practices SCCP that remains ineffective due to missing detailed information of other CPs. Therefore, instead of using SCCP, we employ MCCPs to estimate battery health and life duration. MCCPs boost the efficiency and accurateness of the estimation process through different forms of practicable data.
- To the best of our knowledge, it is the first study that provides a novel comparative study about the data driven-based ML and DL approaches for Li-ion batteries health estimation and remaining effective life duration. The ML methods include SVR, AB while DL models comprise of MLP, CNN, LSTM, and BiLSTM. We apply these approaches with SCCP (V, I, and T are used separately) and combined MCCPs (V, I, and T are used collectively).
- To evaluate the proposed method, we use Li-ion batteries dataset provided by NASA [43] using per cycle capacity and estimation difference. The conducted experiments verify that BiLSTM outperforms other ML and DL approaches.

The organization of the remaining paper is as follows. Section II describes the proposed method for batteries capacity estimation. In Section III, we discuss the experimental results while our conclusion and future directions are given in Section IV of the paper.

II. PROPOSED METHOD

In this section, we discuss the proposed method which consists of three steps as shown in Fig. 1. In preprocessing step, the abnormalities and outliers from the data are removed while in the second step the training procedure is applied using various ML and DL models. In the third step, the final estimation of the battery heath is computed and evaluated using basic error metrics. The subsequent steps of the proposed method are given in the following sections.

A. PREPROCESSING

In order to obtain fine performance, preprocessing is an important step to purify and make the data capable of effective and accurate processing. Initially, there are some outliers and null values in the battery dataset that need refinement before using it for experimentations. The battery dataset consists of four sets of data (where #5, #6, #7, and #18 are the numbers assigned by online repository [43] to the four batteries, respectively) which are chosen for the experimentation. In each set, capacity of the battery is decreasing as cycles are increasing as shown in Fig. 5 (b). According to BMS setting, there are many other points of data during battery charging but there is no need to utilize them for capacity estimation due to complexity and sensitivity. Therefore, first we subsample batteries data in such a way that it reserves the specious variations in charging interval then features are extracted from the subsampled data. We concatenate extracted features from CPs (V, I, and T) to make a 30 dimensional vector where each CP has 10 samples in each vector. According to the model complexity and different variations in CPs with respect to time, the data are resampled into a $n \times 10$ dimensional metric. Next, in a short time interval oscillation prevention, the average of data is calculated over the sampling interval and finally the mean of each CP is concatenated to make final feature vector of length 30. Furthermore, to scale the data between 0 and 1 range for better training process, we apply min-max normalization technique given in equation (1).

$$D_m^n = \frac{z_m^n - \min(Z)}{\max(Z) - \min(Z)} \quad m \in \{1, \ldots, k\} \tag{1}$$

Here, the charging cycle collection is represented by (Z) while (k) shows the number of samples utilized in each cycle. The (D_m^n) is the normalized data in the range of 0 to 1. In addition, the process of de-normalization is also used to present the proposed method estimation in actual form.

B. COVERAGE OF MODELS TRAINING

In training step, we train six various ML and DL approaches separately and attain the best model on the basis of validation data for further evaluation and capacity estimation. These models are AB, SVR, MLP, CNN, LSTM, and BiLSTM which are further explained in the following subsections.

1) MACHINE LEARNING

This section discusses the ML based techniques in details.

A: SUPPORT VECTOR REGRESSION

We use SVR, which is commonly used for regression problems, but uses the same SVM principles. In regression problem, a function can be found on the basis of training samples and that function is used to approximate mapping from an input domain to real number as output. Consider Fig. 2 (a),

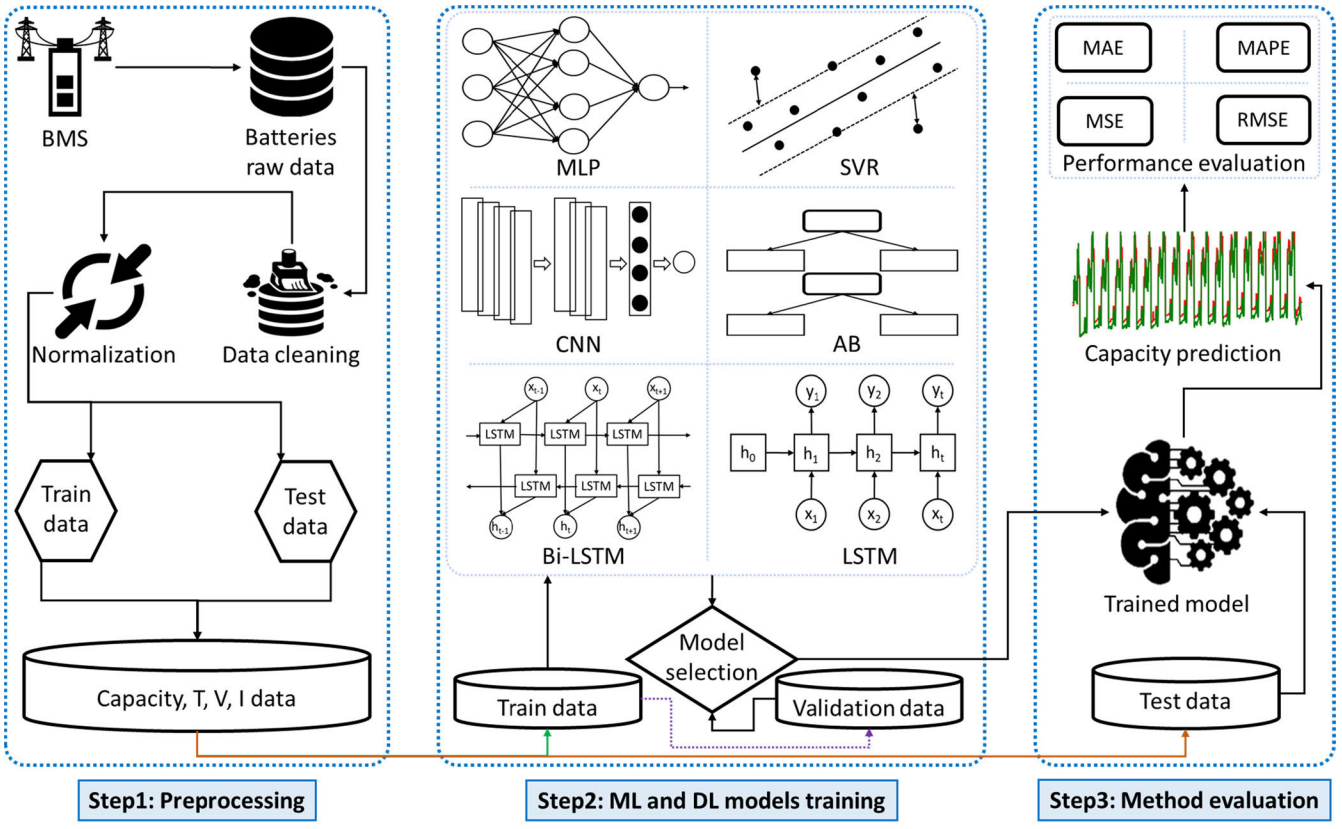

FIGURE 1. Overview of the proposed framework for batteries capacity estimation using MCCPs.

the light-green line is working as the hyperplane while the light-orange two lines are as decision boundary. In SVR the main objective is that it considers only those points that are within the line of decision boundary. A suitable line which has the larger number of points is considered as a hyperplane. To understand the decision boundary, consider the two light-orange lines that are at distance "c" from the hyperplane where the distance can be represented as "+c" and "-c". Assuming if the hyperplane is represented by equation (2) then the equations of decision boundary are represented in equation (3) and (4).

$$y = mz + h \tag{2}$$

$$mz + h = +c \tag{3}$$

$$mz + h = -c \tag{4}$$

Therefore, a hyperplane that satisfies SVR should satisfy equation (5):

$$-c < y - mz + h < +c \tag{5}$$

The primary objective is to establish a decision boundary along the boundary line at "c" distance from the original hyperplane in such a way that data points are nearest to the support vectors or the hyperplane. Therefore, only those points that are within the boundary of the decision and have the lowest rate of error or a tolerance margin are taken into account. This provides us an improved model of fitting.

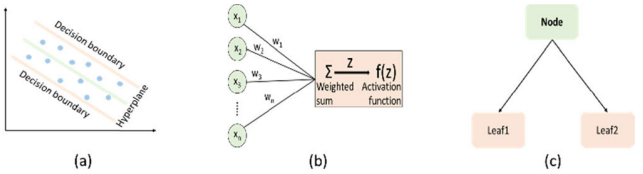

FIGURE 2. (a) Idea behind SVR, (b) Neuron structure, (c) Simple structure of a stump.

B: ADAPTIVE BOOSTING

This section addresses the AB, the short name for the adaptive boosting algorithm that is a boosting approach used as an ensemble method in ML. In each case, the weights are reassigned to wrongly labeled instances with higher weights, so it is called adaptive boosting. To reduce the variance and bias, boosting is used for supervised learning. In this approach, sequential learners are grown where each subsequent learner is grown from previously grown learners except for the first. Using this technique, weak learners can be converted into strong learners. In AB, each node consists of two leaves which are also known as stumps as shown in Fig. 2 (c). The stumps are weak learners, where the order of the stumps is very important since boosting technique prefers it such as in AB. It makes k number of decision trees during the training period of data. As the first decision tree is made, the record which is incorrectly classified during the first

model is given more priority. Only these records are sent as input for the second model. The process will go on until we specify the numbers of base learners that we want to create. Performance of stumps (POS) can be calculated using equation (6), where *ln* is the natural log and TE is the total error which is the sum of all errors in the predicted record for sample weights.

$$\text{POS} = \frac{1}{2}\ln\frac{[1-\text{TE}]}{\text{TE}} \tag{6}$$

2) DEEP LEARNING

This section discusses the techniques based on DL in details.

A: MULTI-LAYER PERCEPTRON

MLP is also known as ANN which mimics the biological brain and is used to solve complex problems like predictive modeling tasks etc. MLP tries to learn mapping i.e. this network has the ability to learn the representation in the training data and its relation with the output data which is to be predicted [44]. It has the ability to learn any mapping function mathematically and is proven to be a generic method of estimation. These networks consist of multi-layered or hierarchical structure due to which they can learn features at different resolutions and scales by providing the combined features of high-order. Artificial neuron (AN) is used as a building block of MLP, where AN is a computational unit that has input with weights and output via an activation function as shown in Fig. 2 (b). Every input feature in AN has a weight value and a bias value than the sum of weighted input features is passed through an activation function like sigmoid, hyperbolic tangent or rectifier, etc. to produce output.

To make MLP neurons are arranged and linked together making an arrangement that is known as the network topology. The arrangement of neurons in a row is called a layer where a MLP has three types of layer, i.e. input or visible, hidden, and output as shown in Fig. 4 (a). The layer which takes input data or features directly is called the visible or input layer. This layer has no weights and activation functions, it just forwards the input data to the next layers. The hidden layer receives feedback from the input layer where in terms of accuracy and complexity, the number of hidden layers and the number of neurons in each hidden layer influence the output of a model. The last layer of the model is called the output layer where its nodes and type of activation function depend on the problem. Normally, the output or last layer has single neuron for single output with linear activation function in case of a regression problem.

B: CONVOLUTIONAL NEURAL NETWORK

CNN is basically designed for object classification and recognition tasks since this network reserves the problem special structure. Nowadays researchers have achieved outstanding performance using CNN in various domains such as crowd analysis [45], violence [46], [47] and anomaly [48] detection, surveillance videos [49] and movies [50] summarization, power consumption prediction [51], [52], and emotions recognition in visual and speech data [53], [54], etc. There are various benefits of the CNN, such as these networks use limited weights than MLP, these models are invariant to the distortion and position of an object in a scene, and these model can learn deep features from data automatically.

Fig. 4 (b) shows that a basic CNN architecture contains three different kinds of layers that are fully-connected, convolutional, and pooling. Convolutional layers consist of filters that produce feature maps. All Filters have their specific receptive fields and work as neurons having input with weights and produce outputs which are called feature maps. The pooling layers reduce the previous layer size of the feature maps. In maximum pooling, the largest value is selected while in average pooling the average value is selected from the receptive field. Normally pooling layers are utilized to diminish the overfitting problem, to reduce feature maps size, and to help in choosing a more generalize representation of features. After feature extraction fully-connected layers are used, where these layers have non-linear activation function. These layers are placed at the end of the network which are normally flat FFNN layers. In the output layer of the network, to predict class probabilities softmax activation and for regression problems linear activation function is used.

C: RECURRENT NEURAL NETWORK

RNN is a popular kind of neural networks that is designed for solving complex sequence learning problems. These networks have loops in connection due to which these networks are capable of adding memory and feedback over time to the network. These networks are capable to learn more complex sequences due to the memory block instead of specific patterns. Followings are the two popular RNN variants that are discussed in the subsections.

1) LONG SHORT-TERM MEMORY NETWORK

LSTM network is one of the well-known types of RNN which obtains contemporary results in several domains including activity and action recognition [55] and medical applications [56], etc. To train RNN, backpropagation is used, which causes exploding and vanishing gradient like problems. LSTM network solves the exploding and vanishing gradient problem using backpropagation through time. Unlike MLP that has neurons, there are memory blocks in the LSTM networks that have a connection with each other in the layers. A block of LSTM consists of three types of gates (forget, input, and output) which makes it smarter than traditional neural networks such as MLP and CNN. The forget, input, and output gates provide a memory to the block where these gates manage the output and state of the block using the sigmoid activation function. The input gate decides conditionally that which values will update the state of memory from the input sequence. The forget gate decides that which information will be discarded conditionally from the block, while the output gate decides based on input and the unit memory conditionally that what to output as shown

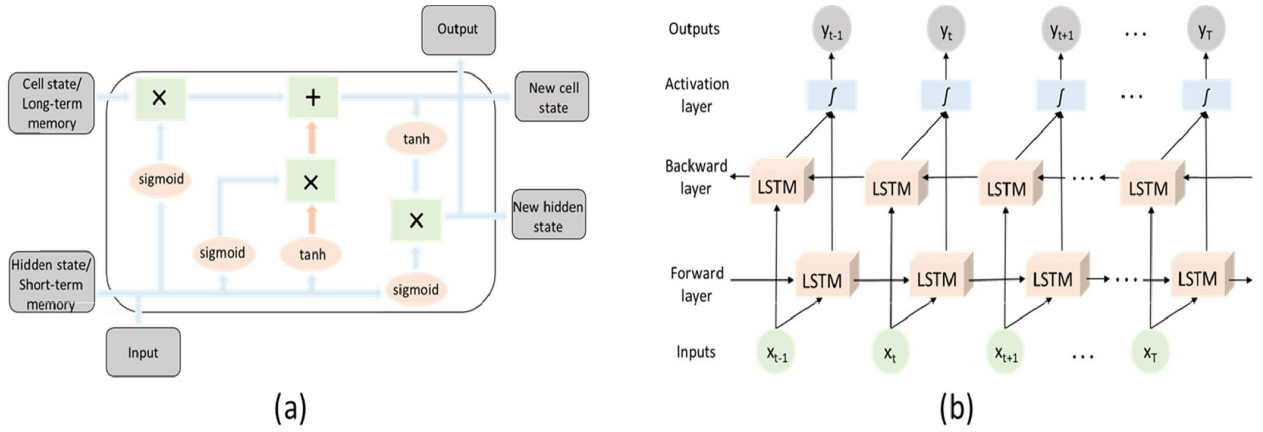

FIGURE 3. (a) The LSTM cell, (b) Working flow of BiLSTM.

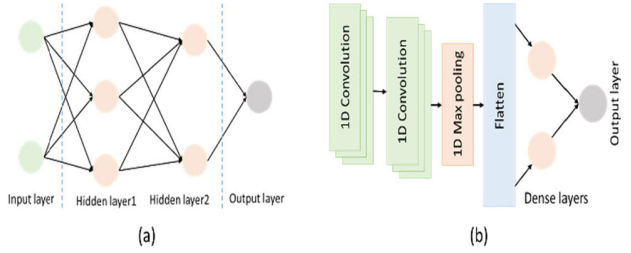

FIGURE 4. (a) MLP architecture, (b) Architecture of 1D CNN.

in Fig. 3 (a). A block works like a state machine while during training the weights are learned for each gate.

2) BI-DIRECTIONAL LSTM NETWORK

BiLSTM networks are the extended form of typical LSTM and their performance is better on sequence related problems. BiLSTM processes the data in both forward and backward directions to keep track of past and future information. For this purpose, instead of one LSTM, two LSTM networks are trained in BiLSTM on the input sequence where all the time steps of the input sequence are available as shown in Fig. 3 (b). Therefore, the results of BiLSTM are faster and accurate due to the adding of additional context to the network. There is a basic idea behind the BiLSTM that involves replicating the first repeated layer in the network and then supplying the input sequence as it is as an input to the first layer and providing a reverse copy of the input sequence to the replicated layer. The restriction of conventional LSTM can be minimized in this way. BiLSTM may use all available input data in training for a particular time phase in the past and in the future.

C. MODELS ARCHITECTURE AND EVALUATION STRATEGY

The validation dataset is used to design and select the architectures of SVR, AB, MLP, CNN, LSTM, and BiLSTM. A model is selected for testing purpose which performs better among all the models on validation dataset. The selected trained model is utilized to predict the capacity for testing data and the performance is evaluated using four error metrics

TABLE 1. The architectures of the proposed DL models and their parameters where I is the input layer, H is the hidden layer, O is the output layer, C is CNN layer, L is the LSTM layer, BL is the BiLSTM layer, and F is the fully-connected layer.

Model name	Model structure	Model parameters
MLP	**I ▶ H1 ▶ H2 ▶ O**	SCCP = 971 MCCPs = 1571
	H1 = 30 neurons	
	H2 = 20 neurons	
CNN	**I ▶ C1 ▶ C2 ▶ F ▶ O**	SCCP = 2161 MCCPs = 5161
	No of Filters = C1(25), C2(15)	
	Filters size = C1(1×3), C2(1×3)	
	Stride = C1(1,1), C2(1,1)	
	F = 10 neurons	
LSTM	**I ▶ L ▶ F ▶ O**	SCCP = 8581 MCCPs = 11781
	Sequence length = 5	
	L = 40 hidden units	
	F = 10 neurons	
BiLSTM	**I ▶ BL ▶ F ▶ O**	SCCP = 17141 MCCPs = 23541
	Sequence length = 5	
	BL = 40 hidden units	
	F = 10 neurons	

including MAE, MSE, RMSE, and MAPE. The architecture of models and their hyper-parameters are given in Table 1. MLP consists of input layer, 2 hidden layers, and output layer with 1 neuron having linear activation function where first hidden layer contains 30 neurons while second hidden layer consists of 20 neurons. Similarly, the proposed architecture of CNN architecture consists of input layer, 2 CNN layers, 1 fully-connected layer having 10 neurons, and output layer with 1 neuron having linear activation function. The filter size is kept same in both CNN layers while first CNN layer having 25 filters, while second CNN layer has 15 filters. LSTM and BiLSTM both have input layer, recurrent layers with 40 hidden units for each layer, fully-connected layer with 10 neurons, and output layer with neuron having linear activation function. Models are evaluated and discussed comprehensively in the experimentation section (3) using NASA

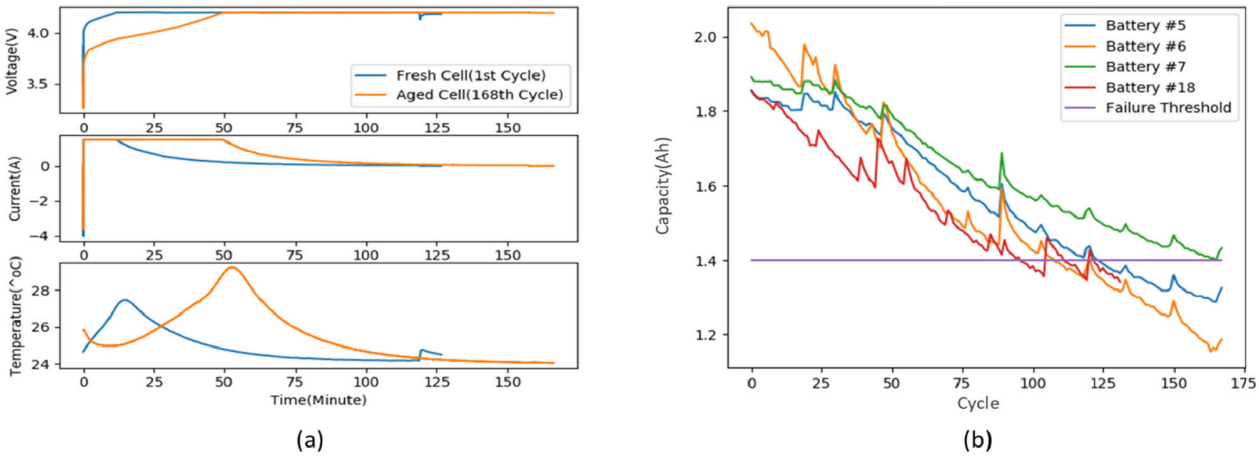

FIGURE 5. (a) CPs such as V, I, and T for fresh cell and aged cell, (b) Capacity degradation with respect to cycles.

battery dataset also, the detail discussion on hyper-parameters is also provided in experimentation section.

III. EXPERIMENTAL RESULTS

In this section, we discuss the experiments obtained for battery capacity estimation, the system configuration, data acquisition, and results comparison of machine learning (ML) and deep learning (DL) based approaches for single channel charging profile (SCCP) and multiple channel charging profiles (MCCPs) in detail. Similarly, we provide a thorough discussion for capacity estimation on the basis of acquired outcomes.

A. DATA SETTINGS

The internal parameters of battery are very critical to estimate battery degradation. Thus, to capture these parameters, the voltage (V), temperature (T), and current (I) data are leveraged and the data at every charging cycle are measured. Three status of battery data are usually used, which are in actual applications. These statuses are charging, discharging, and rest. Measuring or calculating the internal parameters is very hard during discharging process. Similarly, the batteries have usually a peaceable process of charging that are based on preset protocols to measure the electrical performance which is easily measured. Further, the discharging is mainly depending on owner's routine that is changing randomly. There is significant variation to the voltage, current, and temperature profiles when battery ages during charging, which can be easily observed from Fig. 5 (a). During process of charging, the voltage of aged cell reaches 4.2 volt (v) before the voltage of new cell. Similarly, the current of old cell falls down prior than the current of new cell. Furthermore, the old cell has high temperature than the new cell. To easily quantify the battery aging, the state of health (SOH) is formulated that is given in equation (7).

$$\text{SOH}\,(\%) = \frac{C_k}{C_0} \times 100 \tag{7}$$

where C_0 shows capacity while C_k measures the capacity with k cycle. When the battery capacity is below 70%, we determine that the battery life is over.

B. SYSTEM CONFIGURATION

We verified and examined the effectiveness of the proposed method to evaluate its performance via several settings. We implemented the system in python with 3.5 version in Keras and DL framework Tensorflow as a backend by utilizing the Adam optimizer and trained the model for 300 epochs with a batch size of 32. Such a setting ensured to record the smallest metrics error. Initially, 85% and 15% of data are used as training and testing sets for each battery, respectively. Next, we used different combinations of batteries data. Generally, if three batteries data are used as training, the fourth battery data is used as testing set. For instance, battery #5, battery #6, and battery #7 are used as training set while battery #18 is used as testing set. Similarly, in another combination, battery #6, battery #7, and battery #18 are considered as training set while battery #5 is used as testing set. In this way, the same strategy is applied to all the batteries data. As we are dealing to the regression problem, therefore we used four basic metrics to evaluate the models quality, e.g., mean absolute error (MAE), mean square error (MSE), mean absolute percentage error (MAPE), and root mean square error (RMSE). All the metrics are given in equation (8) to equation (11). These metrics are broadly used in prediction problems. Suppose, $y_i^{\sim}$ denotes the predicted capacity of a battery and y_i shows the actual capacity, then equation (8) to (11) describe the MSE, RMSE, MAE, and MAPE, respectively. Furthermore, we used different ML and DL techniques to check the performance of the proposed method.

$$MSE = \frac{1}{n}\sum_{i=1}^{n}(y_i - y_i^{\sim})^2 \tag{8}$$

$$RMSE = \sqrt{MSE} = \sqrt{\frac{1}{n}\sum_{i=1}^{n}(y_i - y_i^{\sim})^2} \tag{9}$$

$$MAE = \frac{1}{n}\sum_{i=1}^{n} | y_i - \tilde{y_i} | \tag{10}$$

$$MAPE = \frac{100\%}{n}\sum | \frac{y_i - \tilde{y_i}}{y_i} | \tag{11}$$

C. DATASET

For a fair evaluation of the proposed method, we used NASA battery dataset that is publicly available and its details is covered in the following sections.

NASA Battery Dataset:

This dataset is based on four Li-ion batteries such as battery #5, #6, #7, and #18 which were run at room temperature using three distinct profiles including impedance, charge, and discharge. The constant mode was set for charging purpose at 1.5 Ampere (A) till the voltage of the battery reaches to 4.2v. Following this, the voltage is kept constant till the charge fell down to 20mA. Next, the discharging process was performed at a persistent value of 2A till the voltage for battery #5, #6, #7, and #18 falls down to 2.7v, 2.5v, 2.2v, and 2.5v, correspondingly. During the collection process, the impedance was measured through electrochemical impedance spectroscopy where the frequency swept to 5khz from 0.1hz. After the continuous charging and discharging process, the aging of the batteries got accelerated while the impedance provided the insight. These experiments were stopped when the batteries hit the end of life criteria, which was 30% decay in a rated volume. For the estimation of RUL and state of the charge, this dataset can also be utilized.

D. ABLATION STUDY

The strategy of parameters selection for each method is same. During experimentation, we used the default values for the two hyper-parameters while altering the third hyper-parameter. Similarly, we apply the same procedure for all the methods of using default values for two hyper-parameters. In this way, we select those hyper-parameters for which we obtain the highest achievable results. For each method, the hyper-parameters are different as their internal network architecture is different. For instance, for adaptive boosting (AB), the hyper-parameters are number of trees, learning rate, and the depth.

On the AB, the MSE value is 2.5879 which is the best achieved results with respect to other hyper-parameters. Similarly, for support vector regression (SVR), the hyper-parameters are type of kernel, regularization, and gamma values. The optimum achieved MSE value on SVR is 2.6181. The hyper-parameters used for multi-layer perceptron (MLP) are epochs, usage of optimization algorithm, and learning rate. Using these parameters, the smallest achieved MSE value is 0.5142. For convolutional neural network (CNN), long short-term memory (LSTM), and bi-directional LSTM (BiLSTM), the hyper-parameters are same. These hyper-parameters are number of epochs, usage of optimization algorithm, and learning rate. Consequently, the MSE values obtained for CNN, LSTM, and BiLSTM are 0.7192, 0.0781, and 0.0317, respectively. Further details of hyper-parameters corresponding to each method are given in Fig. 8, Fig. 9, and Fig. 10.

TABLE 2. Results using various combination of batteries data.

Methods	MSE	RMSE	MAE	MAPE
Battery #5				
SVR	0.8766	0.9363	0.8986	0.9248
AB	0.2884	0.5370	0.4267	0.6873
MLP	0.0011	0.0330	0.0263	0.0493
CNN	0.0023	0.0482	0.0314	0.0514
LSTM	0.0006	0.0251	0.0162	0.0367
BiLSTM	**0.0001**	**0.0099**	**0.0095**	**0.0076**
Battery #6				
SVR	0.9409	0.9700	0.9083	0.9973
AB	0.3577	0.5981	0.4822	0.6993
MLP	0.0015	0.0391	0.0296	0.0504
CNN	0.0024	0.0492	0.0373	0.0585
LSTM	0.0007	0.0272	0.0192	0.0391
BiLSTM	**0.0001**	**0.0110**	**0.0107**	**0.0084**
Battery #7				
SVR	0.9964	0.9982	0.9811	1.1525
AB	0.3614	0.6012	0.5132	0.7545
MLP	0.0017	0.0422	0.0384	0.0590
CNN	0.0026	0.0511	0.0491	0.0614
LSTM	0.0009	0.0296	0.0202	0.0402
BiLSTM	**0.0003**	**0.0182**	**0.0138**	**0.0091**
Battery #18				
SVR	1.4889	1.2202	0.9990	1.1943
AB	0.5220	0.7225	0.5982	0.7970
MLP	0.0023	0.0481	0.0393	0.0604
CNN	0.0034	0.0586	0.0401	0.0690
LSTM	0.0009	0.0302	0.0253	0.0484
BiLSTM	**0.0004**	**0.0190**	**0.0142**	**0.0094**

E. DISCUSSION

This section deeply discusses about the experimental results obtained using SVR, AB, MLP, CNN, LSTM, and BiLSTM. Next, we also discuss the results obtained using both the SCCP and MCCPs while, in MCCPs the capacity is estimated using voltage, current, and temperature collectively. The details are covered in the following paragraphs.

We discuss the evaluation of ML approaches in details such as SVR, AB. At first, we performed experiments over SVR and AB. The SVR works same as SVM but only few differences. Its output is a real number in case of regression problem that becomes difficult for SVR to predict and estimate the battery health. Its further details are given in the previous section. Furthermore, we perform experiments on AB and its detailed description is also given in the previous section. By using best hyper-parameters, the results obtained on SVR and AB using MCCPs are given in Table 4 on every set of battery dataset such as #5, #6, #7, and #18. Similarly, their results obtained over SCCP for voltage, current, and temperature are given in Table 5, Table 6, and Table 7. The MSE values obtained for battery #5, #6, #7, and #18 on SVR for MCCPs are 0.8775, 0.9415, 0.9978, and 1.4908,

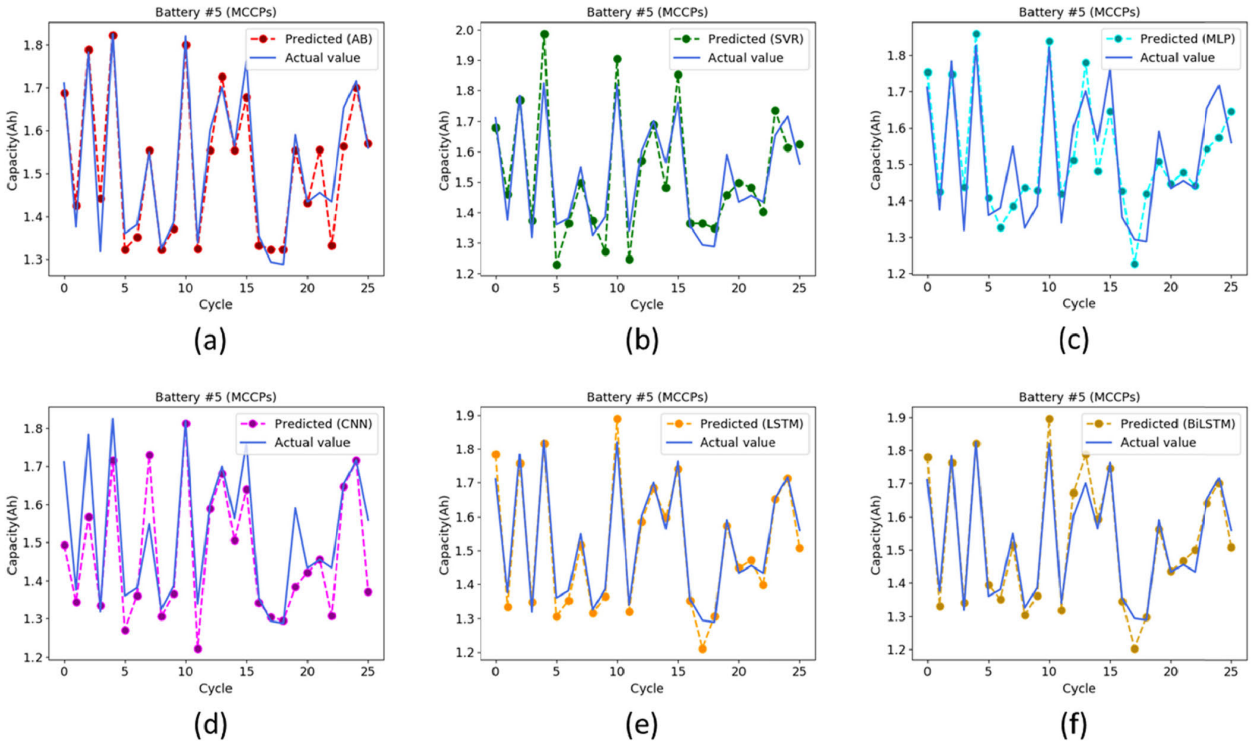

FIGURE 6. Capacity estimation for Battery #5 using MCCPs: (a) AB, (b) SVR, (c) MLP, (d) CNN, (e) LSTM, and (f) BiLSTM.

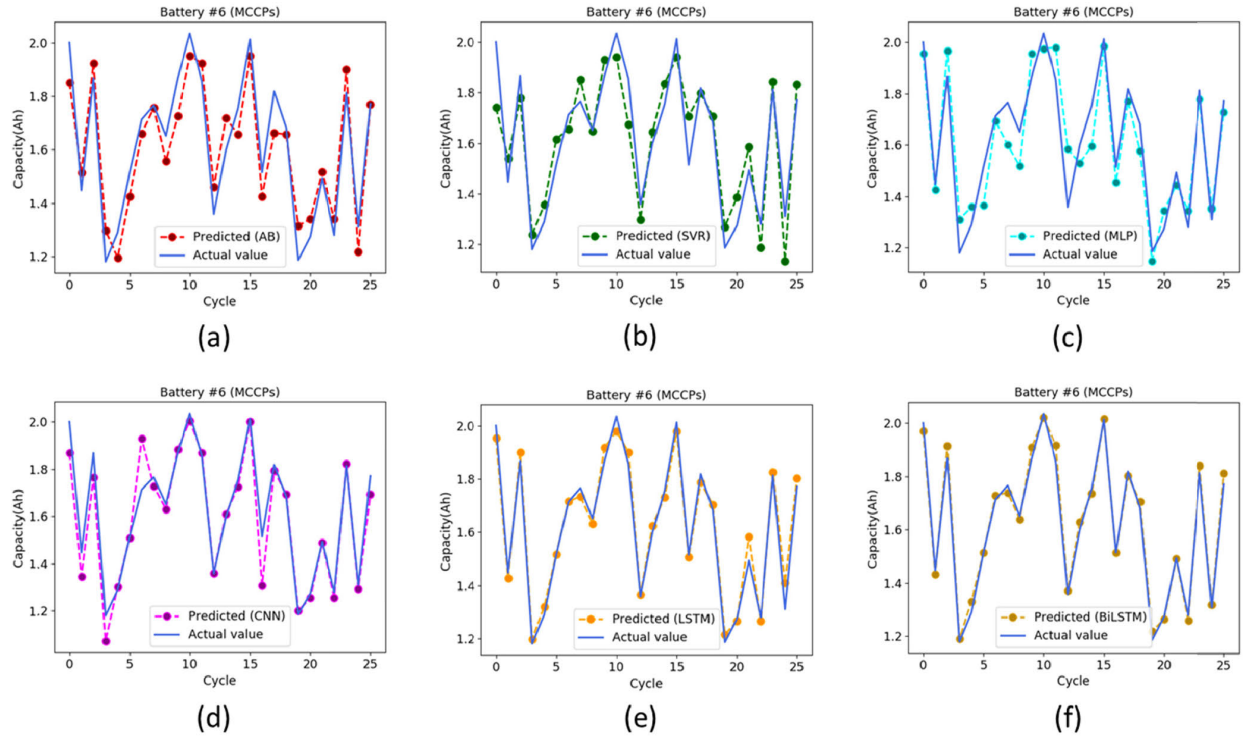

FIGURE 7. Capacity estimation for Battery #6 using MCCPs: (a) AB, (b) SVR, (c) MLP, (d) CNN, (e) LSTM, and (f) BiLSTM.

respectively. Consequently, the MSE values obtained for battery #5, #6, #7, and #18 on AB for MCCPs are 0.2889, 0.3584, 0.3625, and 0.5231, respectively. These results are given in Table 4. Further, we use different size of input sequence to verify the effectiveness of LSTM and BiLSTM. The results obtained using MCCPs with 10×3 sequence and different combinations of datasets are shown in Table 3. On the other hand, the results obtained on SVR, AB, MLP, CNN, LSTM,

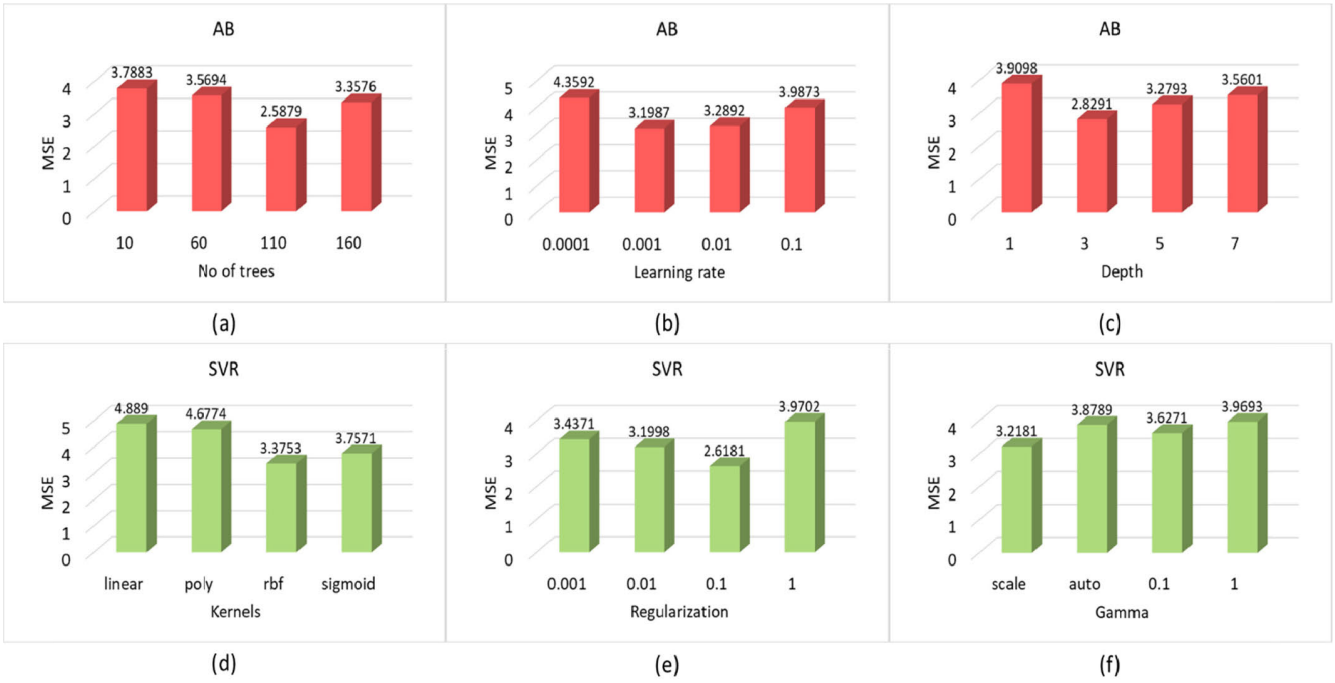

FIGURE 8. AB and SVR hyper-parameters and their corresponding error rates in terms of MSE.

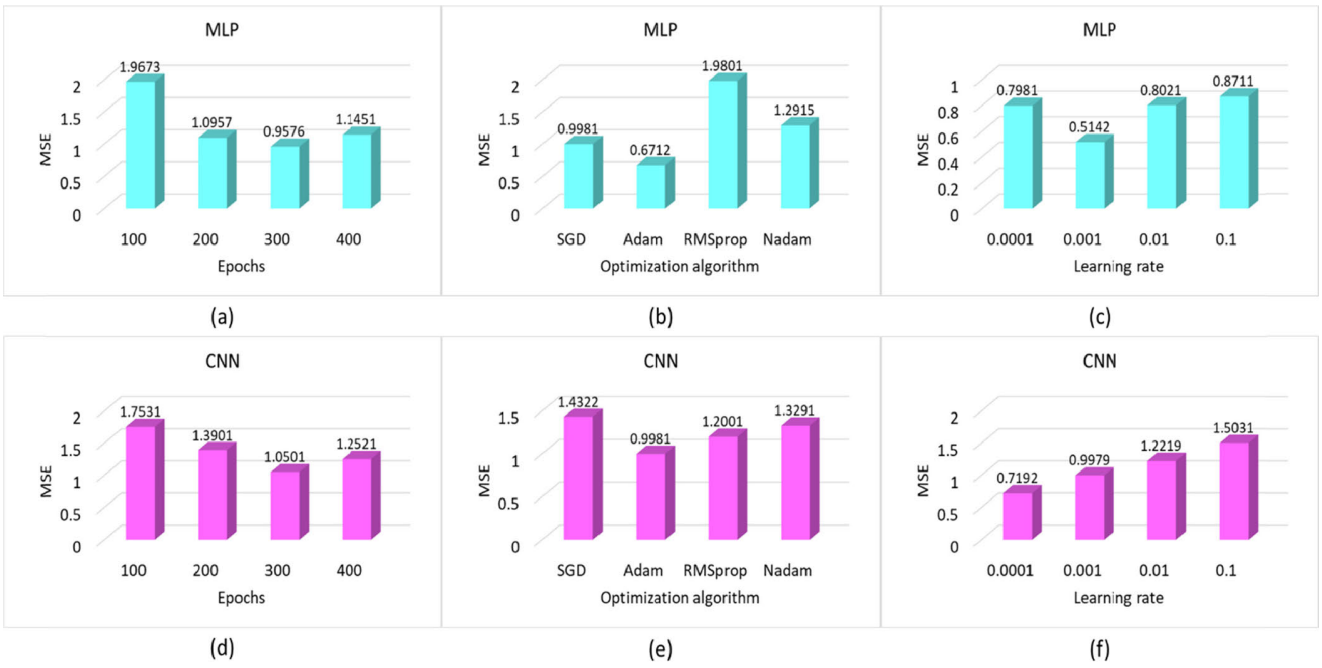

FIGURE 9. MLP and CNN hyper-parameters and their corresponding error rates in terms of MSE.

and BiLSTM using MCCPs and different combinations of datasets are given in Table 2. Similarly, MLP network is used that contains input, hidden, and output layers. The perceptron is a supervised technique that convert the input set into output and acts a linear classifier where the linear predictor performs the job of classification. This classifier combines set of weights with input vector. Similarly, perceptron contains multiple layers connected to each other via directed graph to solve a computational problem. Experiments using MLP are performed for each battery in NASA battery dataset. Table 4 summarize the results using MCCPs for battery #5, #6, #7, and #18 on MLP while its results on SCCP for voltage,

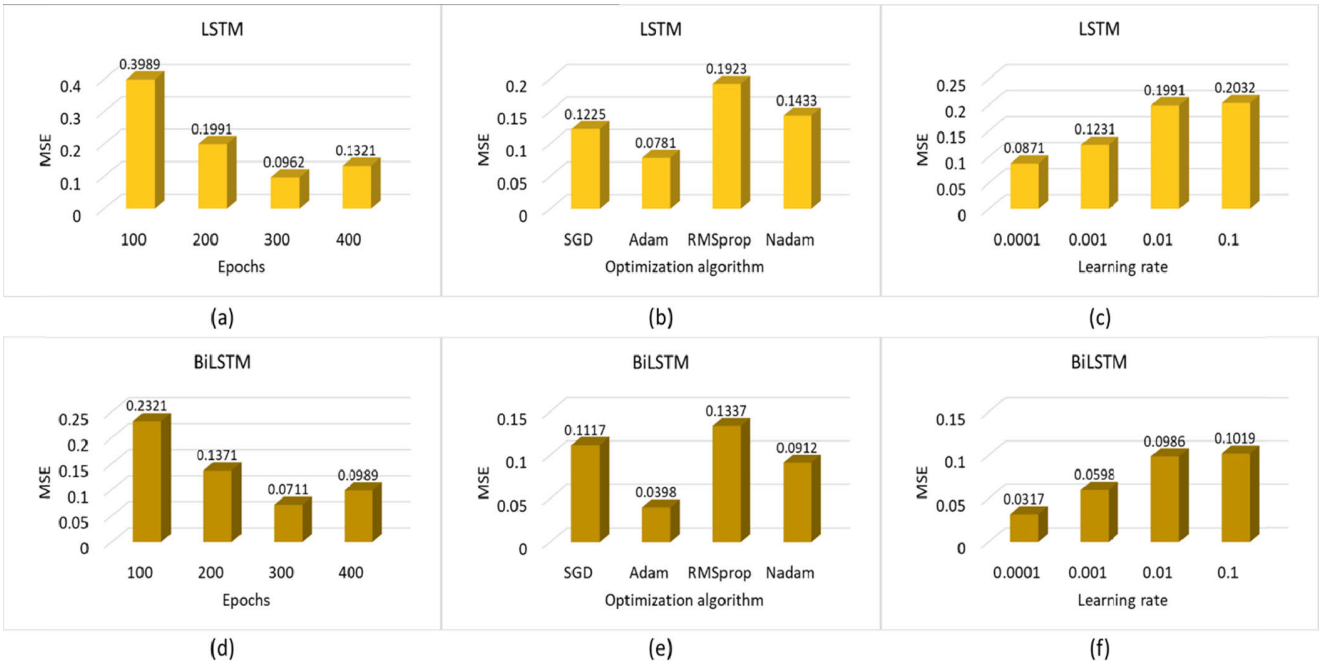

FIGURE 10. LSTM and BiLSTM hyper-parameters and their corresponding error rates in terms of MSE.

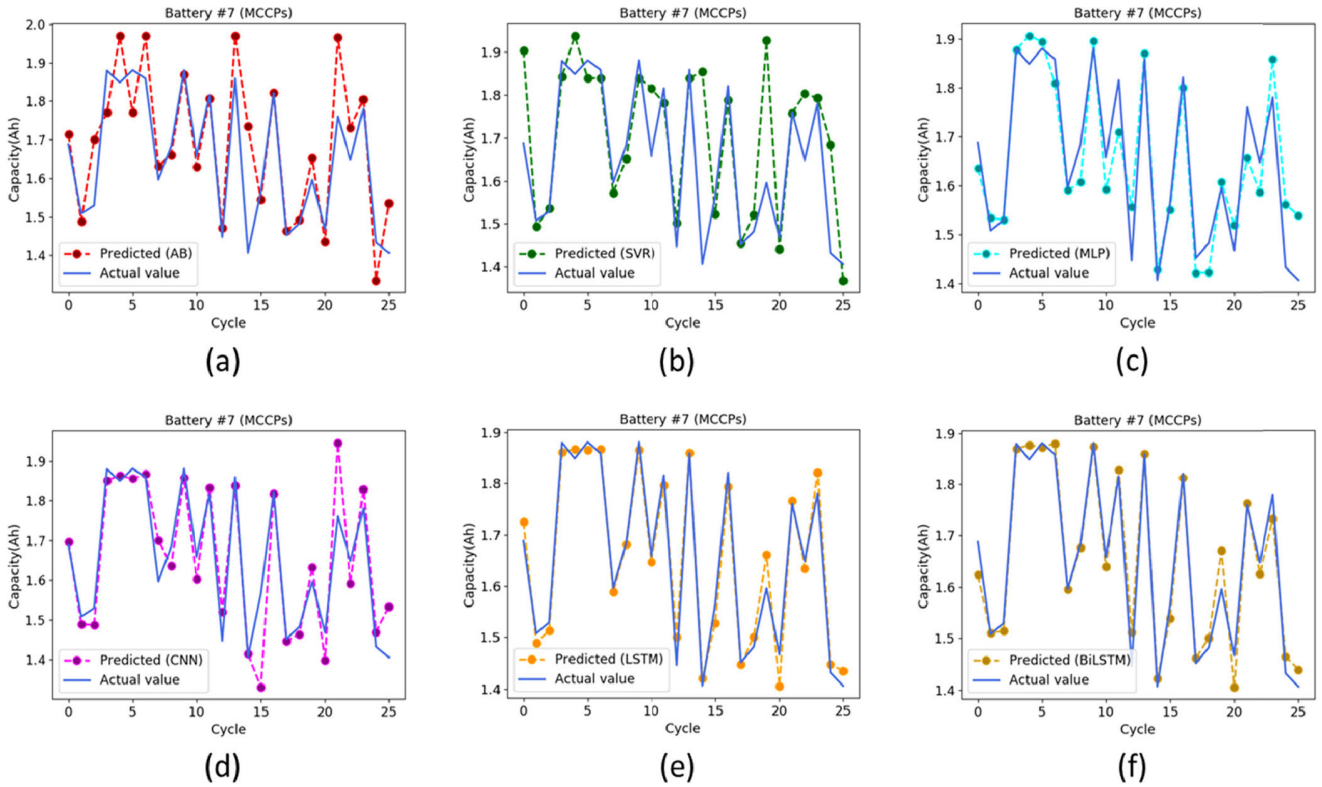

FIGURE 11. Capacity estimation for Battery #7 using MCCPs settings: (a) AB, (b) SVR, (c) MLP, (d) CNN, (e) LSTM, and (f) BiLSTM.

current, and temperature are given in Table 5, Table 6, and Table 7. Compared to the statistical and other hand carried engineering methods, the BiLSTM is proven to be good performer and its experimental details are given in the same section. We plotted the results obtained for battery #5, battery #6, battery #7, and battery #18 using MLP on MCCPs where

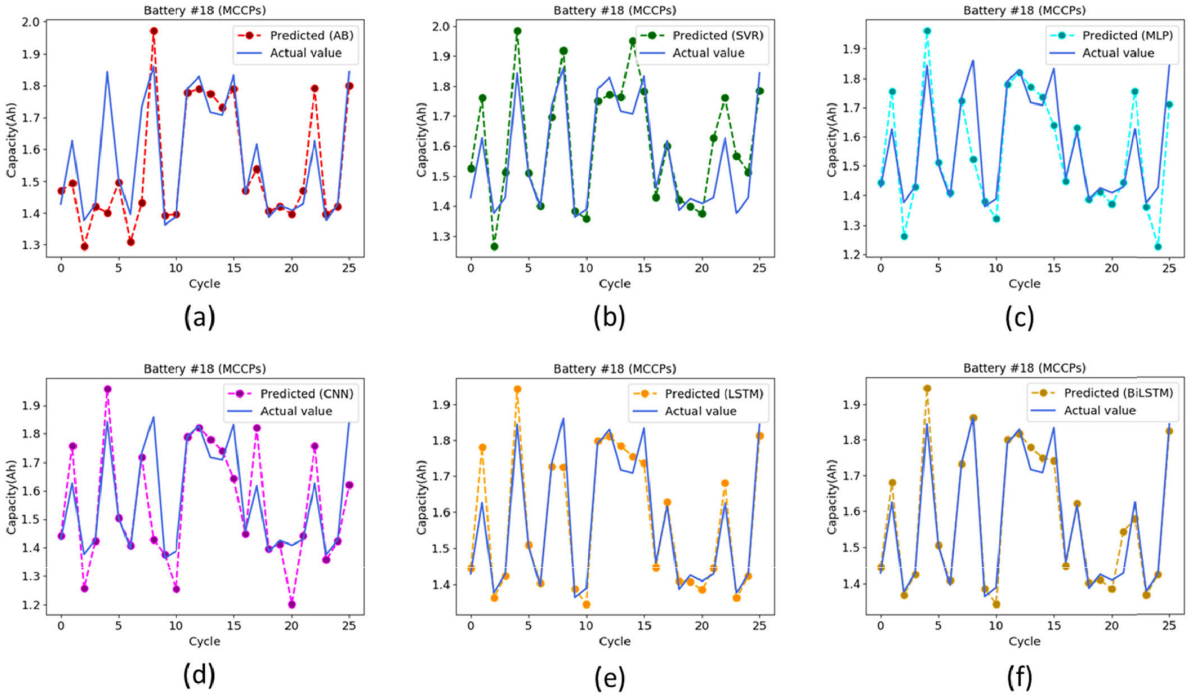

FIGURE 12. Capacity estimation for Battery #18 using MCCPs: (a) AB, (b) SVR, (c) MLP, (d) CNN, (e) LSTM, and (f) BiLSTM.

TABLE 3. 10 × 3 sequence results for LSTM and BiLSTM.

Battery #5				
Methods	**MSE**	**RMSE**	**MAE**	**MAPE**
LSTM	0.0006	0.0249	0.0156	0.0359
BiLSTM	**0.0001**	**0.0099**	**0.0091**	**0.0072**
Battery #6				
LSTM	0.0007	0.0269	0.0176	0.0397
BiLSTM	**0.0001**	**0.0102**	**0.0101**	**0.0078**
Battery #7				
LSTM	0.0005	0.0231	0.0201	0.0402
BiLSTM	**0.0002**	**0.0127**	**0.0122**	**0.0081**
Battery #18				
LSTM	0.0007	0.0281	0.0250	0.0478
BiLSTM	**0.0002**	**0.0129**	**0.0121**	**0.0080**

TABLE 4. Capacity estimation using MCCPs for NASA battery dataset.

Battery #5				
Methods	**MSE**	**RMSE**	**MAE**	**MAPE**
SVR	0.8775	0.9368	0.8991	0.9253
AB	0.2889	0.5375	0.4272	0.6878
MLP	0.0011	0.0335	0.0268	0.0498
CNN	0.0024	0.0487	0.0319	0.0519
LSTM	0.0006	0.0256	0.0167	0.0372
BiLSTM	**0.0001**	**0.0100**	**0.0099**	**0.0081**
Battery #6				
SVR	0.9415	0.9703	0.9089	0.9979
AB	0.3584	0.5987	0.4828	0.6999
MLP	0.0016	0.0397	0.0302	0.0510
CNN	0.0025	0.0498	0.0379	0.0591
LSTM	0.0007	0.0278	0.0198	0.0397
BiLSTM	**0.0001**	**0.0114**	**0.0110**	**0.0090**
Battery #7				
SVR	0.9978	0.9989	0.9818	1.1532
AB	0.3625	0.6021	0.5139	0.7552
MLP	0.0018	0.0431	0.0391	0.0597
CNN	0.0027	0.0518	0.0391	0.0621
LSTM	0.0009	0.0299	0.0209	0.0409
BiLSTM	**0.0004**	**0.0191**	**0.0145**	**0.0098**
Battery #18				
SVR	1.4908	1.2210	0.9998	1.1951
AB	0.5231	0.7233	0.5989	0.7978
MLP	0.0024	0.0489	0.0401	0.0612
CNN	0.0035	0.0594	0.0409	0.0698
LSTM	0.0009	0.0310	0.0261	0.0492
BiLSTM	**0.0004**	**0.0198**	**0.0150**	**0.0102**

the prediction results are shown in Fig. 6, Fig. 7, Fig. 11, and Fig. 12, respectively. Several tasks involving classification or forecasting use univariate or multi-variate data to solve particular problem depending on their applications. Existing literature on CNN has shown promising and outstanding results for both computer vision and time series problems, therefore, to verify and confirm the effectiveness of the proposed method, we also check its performance for capacity estimation. It gives a smooth learning process where first layers are convolutional layers and used to extract features while, pooling layer performing smoothing as they are the part of the same function to give output predictions through optimization of neural network loss. The later layers use smoothed data to handle the time series forecasting. The input layer obtains fixed length of sub-sequence time series and pass it to convolutional layer. Using CNN, we also consider its performance for all the batteries. Its results using MCCPs are briefly given in Table 4 for each battery set. The MSE values obtained for battery #5, #6, #7, and #18 on CNN for MCCPs are 0.0024, 0.0025, 0.0027, and 0.0035, respectively.

TABLE 5. Capacity estimation using SCCP for NASA battery dataset by considering (V).

Battery #5				
Methods	**MSE**	**RMSE**	**MAE**	**MAPE**
SVR	2.1524	1.4671	1.3921	1.6452
AB	0.8303	0.9112	0.9012	0.9912
MLP	0.0040	0.0636	0.0558	0.0366
CNN	0.0059	0.0767	0.0688	0.0443
LSTM	0.0008	0.0289	0.0211	0.0138
BiLSTM	**0.0006**	**0.0241**	**0.0188**	**0.0131**
Battery #6				
SVR	2.1535	1.4675	1.4527	1.6458
AB	0.8310	0.9116	0.9108	0.9917
MLP	0.0041	0.0638	0.0560	0.0368
CNN	0.0060	0.0769	0.0690	0.0446
LSTM	0.0008	0.0291	0.0215	0.0140
BiLSTM	**0.0006**	**0.0244**	**0.0189**	**0.0132**
Battery #7				
SVR	2.1550	1.4680	1.4532	1.6464
AB	0.8321	0.9122	0.9114	0.9923
MLP	0.0041	0.0643	0.0566	0.0372
CNN	0.0060	0.0774	0.0696	0.0449
LSTM	0.0009	0.0294	0.0219	0.0145
BiLSTM	**0.0006**	**0.0248**	**0.0191**	**0.0136**
Battery #18				
SVR	2.1574	1.4688	1.4539	1.6469
AB	0.8330	0.9127	0.9119	0.9927
MLP	0.0041	0.0643	0.0566	0.0372
CNN	0.0061	0.0779	0.0701	0.0454
LSTM	0.0009	0.0299	0.0224	0.0150
BiLSTM	**0.0006**	**0.0252**	**0.0195**	**0.0139**

TABLE 6. Capacity estimation using SCCP for NASA battery dataset by considering (I).

Battery #5				
Methods	**MSE**	**RMSE**	**MAE**	**MAPE**
SVR	2.1529	1.4673	1.4522	1.6455
AB	0.8306	0.9114	0.9103	0.9915
MLP	0.0041	0.0638	0.0559	0.0368
CNN	0.0060	0.0770	0.0689	0.0445
LSTM	0.0008	0.0291	0.0212	0.0140
BiLSTM	**0.0006**	**0.0243**	**0.0189**	**0.0132**
Battery #6				
SVR	2.1544	1.4678	1.4529	1.6462
AB	0.8316	0.9119	0.9110	0.9921
MLP	0.0041	0.0641	0.0562	0.0372
CNN	0.0060	0.0772	0.0692	0.0450
LSTM	0.0009	0.0294	0.0217	0.0144
BiLSTM	**0.0006**	**0.0243**	**0.0191**	**0.0134**
Battery #7				
SVR	2.1553	1.4681	1.4635	1.6466
AB	0.8323	0.9123	0.9112	0.9925
MLP	0.0041	0.0644	0.0569	0.0374
CNN	0.0060	0.0775	0.0699	0.0451
LSTM	0.0009	0.0295	0.0222	0.0147
BiLSTM	**0.0006**	**0.0249**	**0.0194**	**0.0138**
Battery #18				
SVR	2.1585	1.4692	1.4642	1.6471
AB	0.8337	0.9131	0.9122	0.9929
MLP	0.0042	0.0647	0.0569	0.0374
CNN	0.0061	0.0783	0.0704	0.0456
LSTM	0.0009	0.0300	0.0227	0.0152
BiLSTM	**0.0006**	**0.0256**	**0.0198**	**0.0141**

Similarly, we also evaluate it for SCCP such as voltage, current, and temperature and its details are given in Table 5, Table 6, and Table 7, respectively. The estimated capacity is plotted against the actual capacity using CNN for battery set of #5, #6, #7, #8 and is shown in Fig. 6, 7, 11, and 12.

TABLE 7. Capacity estimation using SCCP for NASA battery dataset by considering (T).

Battery #5				
Methods	**MSE**	**RMSE**	**MAE**	**MAPE**
SVR	2.1527	1.4672	1.4620	1.6452
AB	0.8305	0.9113	0.9107	0.9913
MLP	0.0041	0.0637	0.0557	0.0365
CNN	0.0059	0.0769	0.0686	0.0443
LSTM	0.0008	0.0290	0.0210	0.0139
BiLSTM	**0.0005**	**0.0241**	**0.0186**	**0.0130**
Battery #6				
SVR	2.1538	1.4676	1.4627	1.6460
AB	0.8312	0.9117	0.9111	0.9919
MLP	0.0041	0.0639	0.0560	0.0370
CNN	0.0059	0.0770	0.0690	0.0448
LSTM	0.0008	0.0292	0.0215	0.0142
BiLSTM	**0.0006**	**0.0241**	**0.0189**	**0.0132**
Battery #7				
SVR	2.1541	1.4677	1.4531	1.6462
AB	0.8316	0.9119	0.9112	0.9921
MLP	0.0040	0.0640	0.0565	0.0370
CNN	0.0059	0.0771	0.0694	0.0447
LSTM	0.0008	0.0291	0.0218	0.0143
BiLSTM	**0.0006**	**0.0245**	**0.0190**	**0.0134**
Battery #18				
SVR	2.1582	1.4691	1.4641	1.6470
AB	0.8336	0.9130	0.9129	0.9927
MLP	0.0041	0.0646	0.0568	0.0373
CNN	0.0061	0.0782	0.0702	0.0454
LSTM	0.0009	0.0299	0.0225	0.0151
BiLSTM	**0.0007**	**0.0259**	**0.0197**	**0.0140**

LSTM for sequential learning provides good results as it introduces some special units that are known to be memory block in layers that overcome the vanishing gradient problem.

The memory cells are self-connected in the memory blocks. It takes assistance using three gates such as input gate, output gate, and forgot gate. The input gate takes the data and handle its flow inside the memory cell while the output gate keep track of controlling the data flow in the remaining network. At the previous input, the forgot gate selects the cell state and retains its part in the current moment. These three gates are equivalent to multiplying previous data by a number varying between 0 and 1. To compare and verify the effectiveness of proposed method, we performed the experiments on LSTM for both SCCP and MCCPs for all the batteries sets in NASA battery dataset. The MSE values for battery #5, #6, #7, and #18 for MCCPs are 0.0006, 0.0007, 0.0009, and 0.0009, respectively. The results obtained on the basis of MCCPs for all the batteries sets are given in Table 4 while its results on SCCP such as voltage, current, and temperature are given in Table 5, Table 6, and Table 7, respectively. The estimated capacity for each battery is plotted against the actual capacity using LSTM on battery sets #5, #6, #7, #18 is shown in Fig. 6, 7, 11, and 12, respectively.

Finally, we post about the BiLSTM that is overwhelmingly used in several computer vision and time series problems due to its good performance in sequential learning. The BiLSTM network comprises of forward and backward layers to keep information of past and future data. Its further detailed explanation is briefly covered in the proposed section. Unlike other learning approaches, BiLSTM has shown the best results at all. Like the other models, we also evaluate the BiLSTM for SCCP and MCCPs. The results obtained on BiLSTM for MCCPs for each battery set are given in Table 4 while its SCCP results for voltage, current, and temperature are given in Table 5, Table 6, and Table 7, respectively. Similarly, the prediction graphs obtained on BiLSTM for MCCPs are given in Fig. 6, Fig. 7, Fig. 11, and Fig. 12, respectively.

IV. CONCLUSION

Li-ion batteries have been extensively utilized in several applications for instance automobiles, smartphones, and ESS because of their long life of cycles, great power, and energy densities. The price of batteries is high thus, the degradation of capacity is a consideration to be weighed in this situation. Therefore, a desirable way to lengthen the lifetime of a battery is the consideration of batteries capacity degradation that is needed for safety purposes. Hence, its capacity estimation is crucial for decision making and safety just in time. In this article, we presented a method for capacity estimation for Li-ion batteries based on BiLSTM with SCCP and MCCPs. Utilizing NASA battery dataset, the estimation results are analyzed from some different perspectives such as metrics and capacity estimation graphs. Furthermore, we showed that the proposed BiLSTM has obtained reasonable results and outperformed SCCP based techniques. Performance evaluation is carried out by considering the basic metrics such as MSE, RMSE, MAE, and MAPE. Using SCCP and considering temperature, the obtained MSE values for battery #5, #6, #7, and #18, are 0.0005, 0.0006, 0.0006, and 0.0007, respectively. The MSE value obtained on the proposed BiLSTM using MCCPs is 0.0001 while using SCCP it is 0.0006 for voltage, 0.0006 for current, and 0.0005 for temperature using battery #5 data. Furthermore, using MCCPs and various combination of datasets, MSE values for battery #5, #6, #7, and #18, are 0.0001, 0.0001, 0.0003, and 0.0004, respectively while using 10×3 sequences as input, MSE values for these batteries are 0.0001, 0.0001, 0.0002, and 0.0002.

In the future, we intend to consider real-time data from large scale ESS. Next, we plan to observe environmental conditions such as weather, heating, and cooling profiling for better capacity estimation. Similarly, we aim to include edge computing by the inclusions of resource constrained devices like Internet of Thing.

REFERENCES

[1] O. M. Babatunde, J. L. Munda, and Y. Hamam, "A comprehensive state-of-the-art survey on power generation expansion planning with intermittent renewable energy source and energy storage," *Int. J. Energy Res.*, vol. 43, no. 12, pp. 6078–6107, Oct. 2019.

[2] L. A. Wong, V. K. Ramachandaramurthy, P. Taylor, J. B. Ekanayake, S. L. Walker, and S. Padmanaban, "Review on the optimal placement, sizing and control of an energy storage system in the distribution network," *J. Energy Storage*, vol. 21, pp. 489–504, Feb. 2019.

[3] Z. Liu, Z. Jia, C.-M. Vong, J. Han, C. Yan, and M. Pecht, "A patent analysis of prognostics and health management (PHM) innovations for electrical systems," *IEEE Access*, vol. 6, pp. 18088–18107, 2018.

[4] B. Saha, K. Goebel, S. Poll, and J. Christophersen, "Prognostics methods for battery health monitoring using a Bayesian framework," *IEEE Trans. Instrum. Meas.*, vol. 58, no. 2, pp. 291–296, Feb. 2009.

[5] C. Monitoring, *Diagnostics of Machines-Prognostics Part 1: General Guidelines*, Standard ISO13381-1:(e), Directives Part 2, IO f. S, 2004, p. 14.

[6] M. S. Zitouni, H. Bhaskar, J. Dias, and M. E. Al-Mualla, "Advances and trends in visual crowd analysis: A systematic survey and evaluation of crowd modelling techniques," *Neurocomputing*, vol. 186, pp. 139–159, Apr. 2016.

[7] D.-I. Stroe, V. Knap, M. Swierczynski, A.-I. Stroe, and R. Teodorescu, "Operation of a grid-connected lithium-ion battery energy storage system for primary frequency regulation: A battery lifetime perspective," *IEEE Trans. Ind. Appl.*, vol. 53, no. 1, pp. 430–438, Jan. 2017.

[8] Y. Liu, Y. Zhu, and Y. Cui, "Challenges and opportunities towards fast-charging battery materials," *Nature Energy*, vol. 4, no. 7, pp. 540–550, Jul. 2019.

[9] K. Goebel, B. Saha, A. Saxena, J. R. Celaya, and J. P. Christophersen, "Prognostics in battery health management," *IEEE Instrum. Meas. Mag.*, vol. 11, no. 4, pp. 33–40, Aug. 2008.

[10] M. Daigle and C. S. Kulkarni, "End-of-discharge and end-of-life prediction in lithium-ion batteries with electrochemistry-based aging models," in *Proc. AIAA Infotech Aerosp.*, Jan. 2016, p. 2132.

[11] M. Safari and C. Delacourt, "Simulation-based analysis of aging phenomena in a commercial Graphite/$LiFePO_4$ cell," *J. Electrochem. Soc.*, vol. 158, no. 12, p. A1436, 2011.

[12] L. Zhang, X. Hu, Z. Wang, F. Sun, J. Deng, and D. G. Dorrell, "Multiobjective optimal sizing of hybrid energy storage system for electric vehicles," *IEEE Trans. Veh. Technol.*, vol. 67, no. 2, pp. 1027–1035, Feb. 2018.

[13] C. Hu, G. Jain, P. Tamirisa, and T. Gorka, "Method for estimating capacity and predicting remaining useful life of lithium-ion battery," in *Proc. Int. Conf. Prognostics Health Manage.*, Jun. 2014, pp. 1–8.

[14] C. Hu, H. Ye, G. Jain, and C. Schmidt, "Remaining useful life assessment of lithium-ion batteries in implantable medical devices," *J. Power Sources*, vol. 375, pp. 118–130, Jan. 2018.

[15] D. Liu, X. Yin, Y. Song, W. Liu, and Y. Peng, "An on-line state of health estimation of lithium-ion battery using unscented particle filter," *IEEE Access*, vol. 6, pp. 40990–41001, 2018.

[16] G. L. Plett, "Extended Kalman filtering for battery management systems of LiPB-based HEV battery packs," *J. Power Sources*, vol. 134, no. 2, pp. 277–292, Aug. 2004.

[17] A. Guha and A. Patra, "State of health estimation of lithium-ion batteries using capacity fade and internal resistance growth models," *IEEE Trans. Transport. Electrific.*, vol. 4, no. 1, pp. 135–146, Mar. 2018.

[18] E. Walker, S. Rayman, and R. E. White, "Comparison of a particle filter and other state estimation methods for prognostics of lithium-ion batteries," *J. Power Sources*, vol. 287, pp. 1–12, Aug. 2015.

[19] X. Zheng and H. Fang, "An integrated unscented Kalman filter and relevance vector regression approach for lithium-ion battery remaining useful life and short-term capacity prediction," *Rel. Eng. Syst. Saf.*, vol. 144, pp. 74–82, Dec. 2015.

[20] M. A. Patil, P. Tagade, K. S. Hariharan, S. M. Kolake, T. Song, T. Yeo, and S. Doo, "A novel multistage support vector machine based approach for li ion battery remaining useful life estimation," *Appl. Energy*, vol. 159, pp. 285–297, Dec. 2015.

[21] Y. Li, S. Zhong, Q. Zhong, and K. Shi, "Lithium-ion battery state of health monitoring based on ensemble learning," *IEEE Access*, vol. 7, pp. 8754–8762, 2019.

[22] D. Liu, J. Zhou, H. Liao, Y. Peng, and X. Peng, "A health indicator extraction and optimization framework for lithium-ion battery degradation modeling and prognostics," *IEEE Trans. Syst., Man, Cybern., Syst.*, vol. 45, no. 6, pp. 915–928, Jun. 2015.

[23] J. Wu, C. Zhang, and Z. Chen, "An online method for lithium-ion battery remaining useful life estimation using importance sampling and neural networks," *Appl. Energy*, vol. 173, pp. 134–140, Jul. 2016.

[24] G.-W. You, S. Park, and D. Oh, "Diagnosis of electric vehicle batteries using recurrent neural networks," *IEEE Trans. Ind. Electron.*, vol. 64, no. 6, pp. 4885–4893, Jun. 2017.
[25] X. Hu, J. Jiang, D. Cao, and B. Egardt, "Battery health prognosis for electric vehicles using sample entropy and sparse Bayesian predictive modeling," *IEEE Trans. Ind. Electron.*, vol. 63, no. 4, pp. 2645–2656, Apr. 2016.
[26] S. Shen, M. Sadoughi, X. Chen, M. Hong, and C. Hu, "A deep learning method for online capacity estimation of lithium-ion batteries," *J. Energy Storage*, vol. 25, Oct. 2019, Art. no. 100817.
[27] K. A. Severson, P. M. Attia, N. Jin, N. Perkins, B. Jiang, Z. Yang, M. H. Chen, M. Aykol, P. K. Herring, D. Fraggedakis, M. Z. Bazant, S. J. Harris, W. C. Chueh, and R. D. Braatz, "Data-driven prediction of battery cycle life before capacity degradation," *Nature Energy*, vol. 4, no. 5, pp. 383–391, May 2019.
[28] R. R. Richardson, M. A. Osborne, and D. A. Howey, "Battery health prediction under generalized conditions using a Gaussian process transition model," *J. Energy Storage*, vol. 23, pp. 320–328, Jun. 2019.
[29] J. Shen and A. Khaligh, "A supervisory energy management control strategy in a battery/ultracapacitor hybrid energy storage system," *IEEE Trans. Transport. Electrific.*, vol. 1, no. 3, pp. 223–231, Oct. 2015.
[30] B. Bole, C. S. Kulkarni, and M. Daigle, "Adaptation of an electrochemistry-based li-ion battery model to account for deterioration observed under randomized use," SGT, Moffett Field, CA, USA, Tech. Rep., Oct. 2014.
[31] W. He, N. Williard, C. Chen, and M. Pecht, "State of charge estimation for li-ion batteries using neural network modeling and unscented Kalman filter-based error cancellation," *Int. J. Electr. Power Energy Syst.*, vol. 62, pp. 783–791, Nov. 2014.
[32] E. Reihani, S. Sepasi, L. R. Roose, and M. Matsuura, "Energy management at the distribution grid using a battery energy storage system (BESS)," *Int. J. Electr. Power Energy Syst.*, vol. 77, pp. 337–344, May 2016.
[33] M. Lee, J. Park, S.-I. Na, H. S. Choi, B.-S. Bu, and J. Kim, "An analysis of battery degradation in the integrated energy storage system with solar photovoltaic generation," *Electronics*, vol. 9, no. 4, p. 701, Apr. 2020.
[34] Z. Wei, D. Zhao, H. He, W. Cao, and G. Dong, "A noise-tolerant model parameterization method for lithium-ion battery management system," *Appl. Energy*, vol. 268, Jun. 2020, Art. no. 114932.
[35] Z. Wei, J. Zhao, D. Ji, and K. J. Tseng, "A multi-timescale estimator for battery state of charge and capacity dual estimation based on an online identified model," *Appl. Energy*, vol. 204, pp. 1264–1274, Oct. 2017.
[36] S. Shen, M. Sadoughi, M. Li, Z. Wang, and C. Hu, "Deep convolutional neural networks with ensemble learning and transfer learning for capacity estimation of lithium-ion batteries," *Appl. Energy*, vol. 260, Feb. 2020, Art. no. 114296.
[37] Y. Wang, J. Tian, Z. Sun, L. Wang, R. Xu, M. Li, and Z. Chen, "A comprehensive review of battery modeling and state estimation approaches for advanced battery management systems," *Renew. Sustain. Energy Rev.*, vol. 131, Oct. 2020, Art. no. 110015.
[38] A. Garg, X. Peng, M. L. P. Le, K. Pareek, and C. M. M. Chin, "Design and analysis of capacity models for lithium-ion battery," *Measurement*, vol. 120, pp. 114–120, May 2018.
[39] C. Vidal, P. Malysz, P. Kollmeyer, and A. Emadi, "Machine learning applied to electrified vehicle battery state of charge and state of health estimation: State-of-the-Art," *IEEE Access*, vol. 8, pp. 52796–52814, 2020.
[40] A. Garg, V. Vijayaraghavan, J. Zhang, S. Li, and X. Liang, "Design of robust battery capacity model for electric vehicle by incorporation of uncertainties," *Int. J. Energy Res.*, vol. 41, no. 10, pp. 1436–1451, Aug. 2017.
[41] A. Farmann, W. Waag, A. Marongiu, and D. U. Sauer, "Critical review of on-board capacity estimation techniques for lithium-ion batteries in electric and hybrid electric vehicles," *J. Power Sources*, vol. 281, pp. 114–130, May 2015.
[42] K. B. Hatzell, A. Sharma, and H. K. Fathy, "A survey of long-term health modeling, estimation, and control of lithium-ion batteries: Challenges and opportunities," in *Proc. Amer. Control Conf. (ACC)*, Jun. 2012, pp. 584–591.
[43] B. Saha and K. Goebel, "Battery data set," AMES Prognostics Data Repository, NASA, Washington, DC, USA, Tech. Rep., 2007.
[44] M. Sajjad, S. U. Khan, N. Khan, I. U. Haq, A. Ullah, M. Y. Lee, and S. W. Baik, "Towards efficient building designing: Heating and cooling load prediction via multi-output model," *Sensors*, vol. 20, no. 22, p. 6419, Nov. 2020.
[45] N. Khan, A. Ullah, I. U. Haq, V. G. Menon, and S. W. Baik, "SD-net: Understanding overcrowded scenes in real-time via an efficient dilated convolutional neural network," *J. Real-Time Image Process.*, pp. 1–15, Sep. 2020, doi: 10.1007/s11554-020-01020-8.
[46] F. U. M. Ullah, A. Ullah, K. Muhammad, I. U. Haq, and S. W. Baik, "Violence detection using spatiotemporal features with 3D convolutional neural network," *Sensors*, vol. 19, no. 11, p. 2472, May 2019.
[47] S. U. Khan, I. U. Haq, S. Rho, S. W. Baik, and M. Y. Lee, "Cover the violence: A novel deep-learning-based approach towards violence-detection in movies," *Appl. Sci.*, vol. 9, no. 22, p. 4963, Nov. 2019.
[48] W. Ullah, A. Ullah, I. U. Haq, K. Muhammad, M. Sajjad, and S. W. Baik, "CNN features with bi-directional LSTM for real-time anomaly detection in surveillance networks," *Multimedia Tools Appl.*, pp. 1–17, Aug. 2020, doi: 10.1007/s11042-020-09406-3.
[49] T. Hussain, K. Muhammad, A. Ullah, J. D. Ser, A. H. Gandomi, M. Sajjad, S. W. Baik, and V. H. C. de Albuquerque, "Multi-view summarization and activity recognition meet edge computing in IoT environments," *IEEE Internet Things J.*, early access, Sep. 29, 2020, doi: 10.1109/JIOT.2020.3027483.
[50] I. U. Haq, K. Muhammad, A. Ullah, and S. W. Baik, "DeepStar: Detecting starring characters in movies," *IEEE Access*, vol. 7, pp. 9265–9272, 2019.
[51] F. U. M. Ullah, A. Ullah, I. U. Haq, S. Rho, and S. W. Baik, "Short-term prediction of residential power energy consumption via CNN and multi-layer bi-directional LSTM networks," *IEEE Access*, vol. 8, pp. 123369–123380, 2020.
[52] Z. Khan, T. Hussain, A. Ullah, S. Rho, M. Lee, and S. Baik, "Towards efficient electricity forecasting in residential and commercial buildings: A novel hybrid CNN with a LSTM-AE based framework," *Sensors*, vol. 20, no. 5, p. 1399, Mar. 2020.
[53] S. Kwon, "A CNN-assisted enhanced audio signal processing for speech emotion recognition," *Sensors*, vol. 20, no. 1, p. 183, Dec. 2019.
[54] M. Sajjad, M. Nasir, F. U. M. Ullah, K. Muhammad, A. K. Sangaiah, and S. W. Baik, "Raspberry pi assisted facial expression recognition framework for smart security in law-enforcement services," *Inf. Sci.*, vol. 479, pp. 416–431, Apr. 2019.
[55] A. Ullah, K. Muhammad, J. Del Ser, S. W. Baik, and V. H. C. de Albuquerque, "Activity recognition using temporal optical flow convolutional features and multilayer LSTM," *IEEE Trans. Ind. Electron.*, vol. 66, no. 12, pp. 9692–9702, Dec. 2019.
[56] S. U. Khan and R. Baik, "MPPIF-net: Identification of plasmodium falciparum parasite mitochondrial proteins using deep features with multilayer Bi-directional LSTM," *Processes*, vol. 8, no. 6, p. 725, Jun. 2020.

NOMAN KHAN (Student Member, IEEE) received the bachelor's degree in computer science from Islamia College University Peshawar, Peshawar, Pakistan. He is currently pursuing the M.S. degree in software convergence with Sejong University, Seoul, Republic of Korea. He is currently a Research Assistant with the Intelligent Media Laboratory. His research interests include feature extraction, content-based image retrieval, crowd analysis, virtual and augmented reality, power energy consumption prediction, IoT, IIoT, and resource constrained programming.

FATH U MIN ULLAH (Student Member, IEEE) received the bachelor's degree in computer science from Islamia College University Peshawar, Peshawar, Pakistan. He is currently pursuing the M.S. degree leading to Ph.D. degree with the Intelligent Media Laboratory, Sejong University, Seoul, South Korea. His research interests include computer vision techniques, violence detection, deep learning, image processing, power energy consumption prediction, smart grid, surveillance video analysis, and facial expression recognition. He has authored or coauthored several articles in reputed peer-reviewed international journals, such IEEE Access, *Elsevier Information Science*, and *MDPI SENSORS*. He has expertise in embedded devices, such as raspberry pi. He is also serving as a Reviewer in several well-reputed journals, such as IEEE Access, *Applied Soft-Computing*, the IEEE E*merging* T*opic in* C*omputational* I*ntelligence*, and the *Journal of Visual Communication and Image Representation*. https://publons.com/researcher/3656900/fath-u-min-ullah/.

AFNAN received the bachelor's degree in computer science from Islamia College Peshawar, Peshawar, Pakistan. He is currently a Research Assistant with the Digital Image Processing Laboratory (DIP Lab), Islamia College Peshawar. His research interests include energy data analysis, power energy and load forecasting, image and video analysis, disaster management, crowd analysis, and virtual and augmented reality.

AMIN ULLAH (Member, IEEE) received the Ph.D. degree in digital contents from Sejong University, South Korea. He is currently working as a Postdoctoral Researcher with the Intelligent Media Laboratory, Department of Software, Sejong University. He has published several articles in reputed peer-reviewed international journals and conferences, including IEEE Transactions on Industrial Electronics, IEEE Transactions on Industrial Informatics, IEEE Transactions on Intelligent Transportation Systems, IEEE Internet of Things Journal, IEEE Access, *Future Generation Computer Systems* (Elsevier), *MDPI Sensors*, *Multimedia Tools and Applications* (Springer), *Mobile Networks and Applications* (Springer), and IEEE Joint Conference on Neural Networks. His major research focus is on human action and activity recognition, sequence learning, image and video analytics, content-based indexing and retrieval, IoT and smart cities, and deep learning for multimedia understanding.

MI YOUNG LEE (Member, IEEE) received the M.S. and Ph.D. degrees from the Department of Image and Information Engineering, Pusan National University. She is currently a Research Professor with Sejong University and provide research services at the Intelligent Media Laboratory (IMLab). She is broadly working in artificial intelligence, computer vision, image processing, and energy informatics. Her particular research interests include video summarization, movies data analysis, electrical energy forecasting, and video retrieval. She has published several novel contributions in these areas in reputed journals and peer-reviewed conference proceedings, including IEEE Access, *MDPI Sensors*, *Multimedia Tools and Applications* (Springer), and International Joint Conference on Neural Networks-2020. She has carried out several research projects successfully and is a principal investigator of several ongoing research projects under the supervision of Korean Government and has filed more than five patents during her career.

SUNG WOOK BAIK (Senior Member, IEEE) received the B.S. degree in computer science from Seoul National University, Seoul, South Korea, in 1987, the M.S. degree in computer science from Northern Illinois University, Dekalb, in 1992, and the Ph.D. degree in information technology engineering from George Mason University, Fairfax, VA, USA, in 1999. He was a Senior Scientist with the Intelligent Systems Group, Datamat Systems Research Inc., from 1997 to 2002. In 2002, he joined the faculty of the College of Electronics and Information Engineering, Sejong University, Seoul, where he is currently a Full Professor and the Chief of the Sejong Industry-Academy Cooperation Foundation. He is also the Head of the Intelligent Media Laboratory, Sejong University. His research interests include computer vision, multimedia, pattern recognition, machine learning, data mining, virtual reality, and computer games.